Electronic Supplementary Material (ESI) for Journal of Materials Chemistry C.

Tuning quantum interference through molecular junctions formed from cross-linked OPE-3 dimers.

Bashayr Alanazi[a,b], Asma Alajmi[a,c], Alaa Aljobory[a,d], Colin Lambert[a] and Ali Ismael[a,e*]

Table of contents

1. Optimised DFT Structures of Isolated Molecular-scale Structures.

We used the SIESTA code to calculate the optimised geometries. All molecules shown in Figs. S1 and S2 were relaxed to achieve their optimum geometries, which happens when all forces are less than 0.01eV. A real-space grid is defined by a double-polarized basis set (DZP) with a 250 Ry equivalent energy cutoff. The generalised gradient approximation (GGA) is selected to be the exchange-correlation functional. Fig. S1 shows fully relaxed geometries of the five building blocks used later to create OPE dimers, while Fig. S2 shows fully relaxed geometries of the four dimers.

.

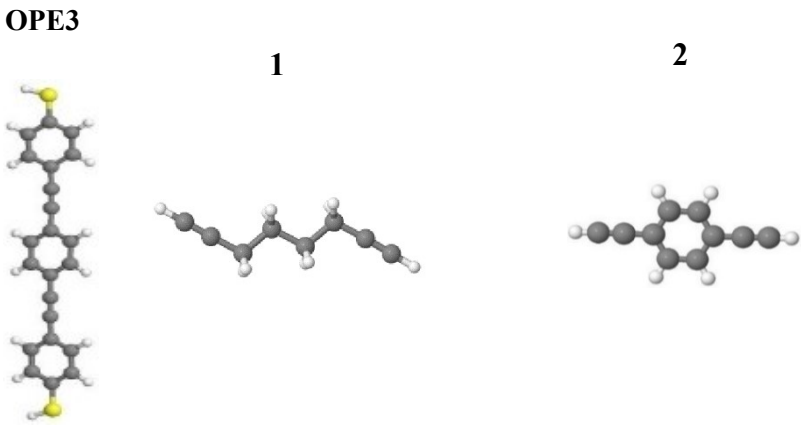

Figure S1: Fully relaxed isolated building blocks used below to create OPE3 dimers.

The following four molecular structures were cross-linked by bridging the components **1** and **2** with OPE Fig. S1, and then allowing the system to become fully relaxed to form cross-linked dimers as shown in Fig. S2.

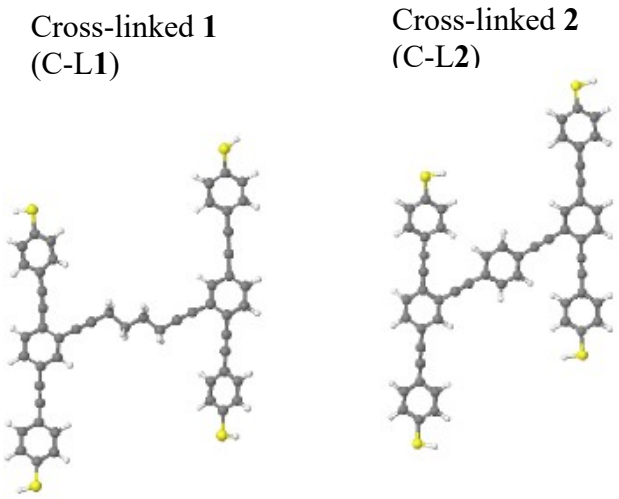

Figure S2: Schematic illustrations of OPE3 dimers bridged by **1** and **2** components of Fig. S1.

2. Frontier molecular orbitals

To have a better understanding of the electronic properties of the molecules in Figs. S1 and S2, the gas-phase electronic structures of all cross-linking were investigated to explore the distribution and composition of the frontier molecular orbitals**.** Plots of the frontier orbitals for the OPE cross-linked dimers are given in Figs. S3-S4, which show the highest occupied molecular orbitals (HOMO) and lowest unoccupied orbitals (LUMO), (HOMO-1), and (LUMO+1), (HOMO-2), and (LUMO+2) along with their energies. The blue and red colours represent the positive and negative orbital amplitudes respectively.

2.1 Cross-linked (1)

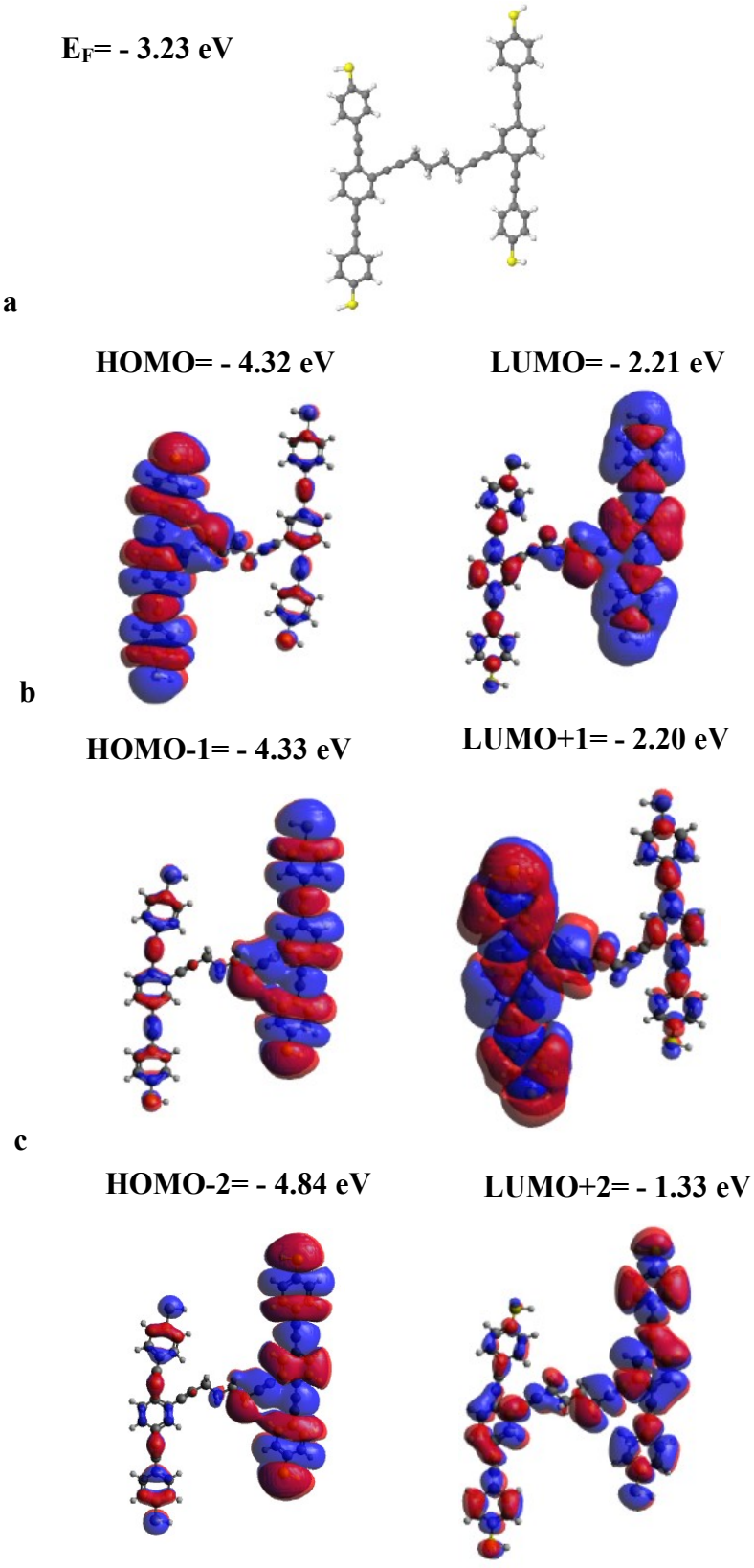

Figure S3: Wave function for cross-linked dimer **1**. **Top panel**: fully optimised geometry of C-L**1**. **Lower panel**: HOMO, LUMO, HOMO-1, LUMO+1, HOMO-2, LUMO+2 of cross-linked **1**, along with their energies.

2.2 Cross-linked (2)

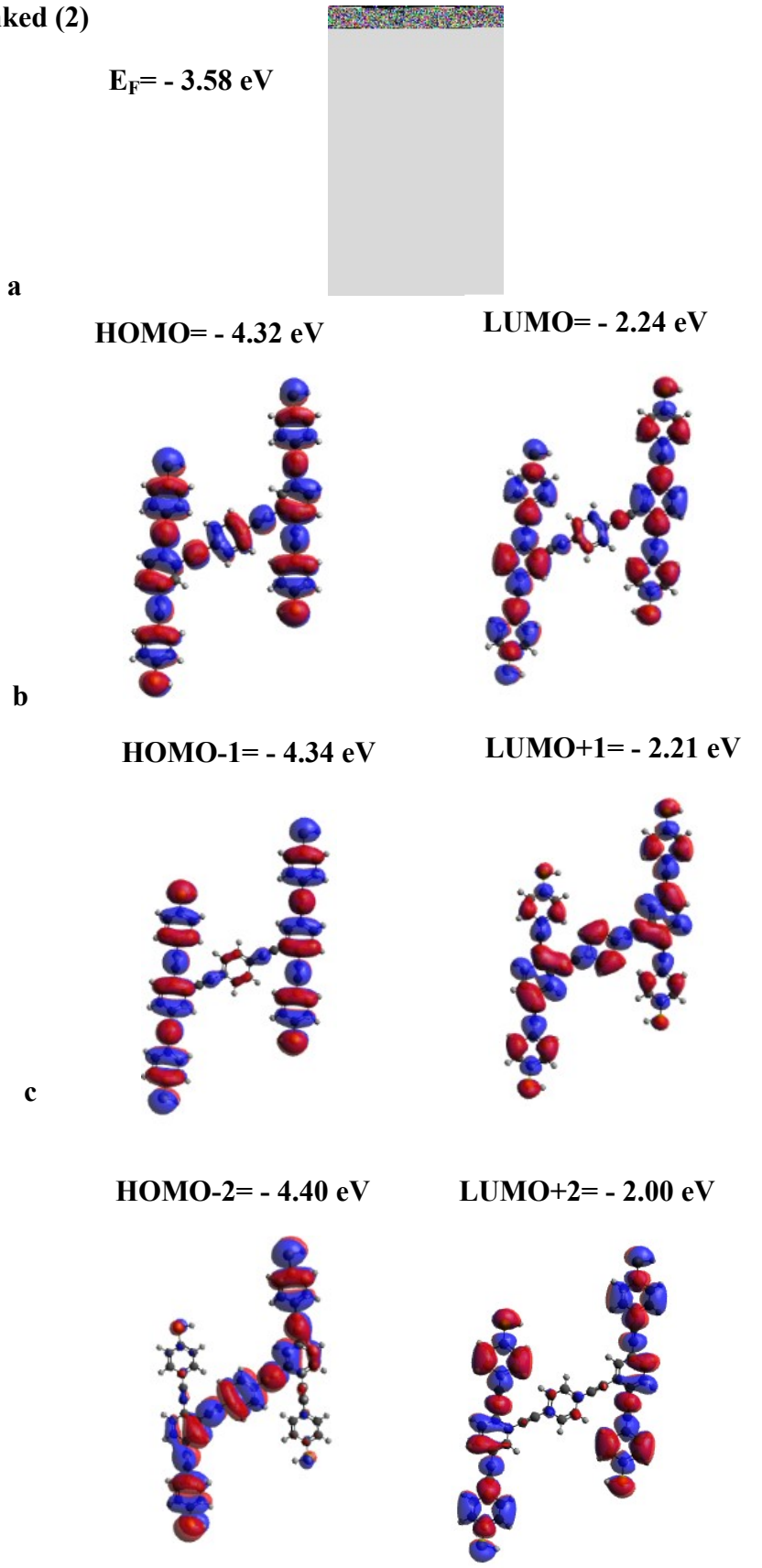

Figure S4: Wave function for cross-linked dimer **2**. **Top panel**: fully optimised geometry of C-L **2**. **Lower panel**: HOMO, LUMO, HOMO-1, LUMO+1, HOMO-2, LUMO+2 of cross-linked **2**, along with their energies.

3. Tight binding model (TBM)

Here, we construct a Hückel (i.e., tight binding, TB) Hamiltonian,[17-19] which characterises the two-contact points dependence of the conductance for the four cross-linked dimers that shown in Fig. 1 of the main paper. The Hamiltonian matrix comprises diagonal elements $H_{jj}= \varepsilon_j$, which describe the energy ε_j of an electron on site j and nearest neighbour off-diagonal elements H_{ij}, which include hopping integrals between neighbouring sites l and j. All other matrix elements are set to zero. If all the sites were identical, then the simplest model would be obtained by setting all $\varepsilon_j=0$ (which defines the zero of energy) and all nearest neighbour coupling equal to -1, which sets the energy scale. Such a Hamiltonian is a simple connectivity table, whose entries H_{ij} are equal to -1 when two atoms i and j are connected and are zero otherwise.

When semi-infinite one-dimensional crystalline leads are coupled to sites **1** and **3**, the $T(E)$ is shown as the red-solid curve in Fig. S5, which clearly exhibits a constructive quantum interference (CQI). Similarly, coupling to sites **2** and **4**, exhibits CQI as indicated by the red-dotted curve. On the other hand, when crystalline leads are linked to sites **1** and **2** or **3** and **4**, the green-solid/-dotted curves are produced and possess a DQI signature (i.e., dip).[20-26] Moving to sites **1** and **4** the purple- sold curve is produced and possesses no DQI signature (i.e., CQI), whereas sites **2** and **3**, the light green-sold curve is produced and possesses a DQI dip. These results for the alkane chain bridged dimer **1**. Tight binding transmission coefficients of cross-linked dimers **1** and **2** demonstrate that the bridging linker has no influence on the transmission curve as the two dimers exhibit roughly the same curves at the 6 different pairs of contacts as shown in Figs. S5-S6).

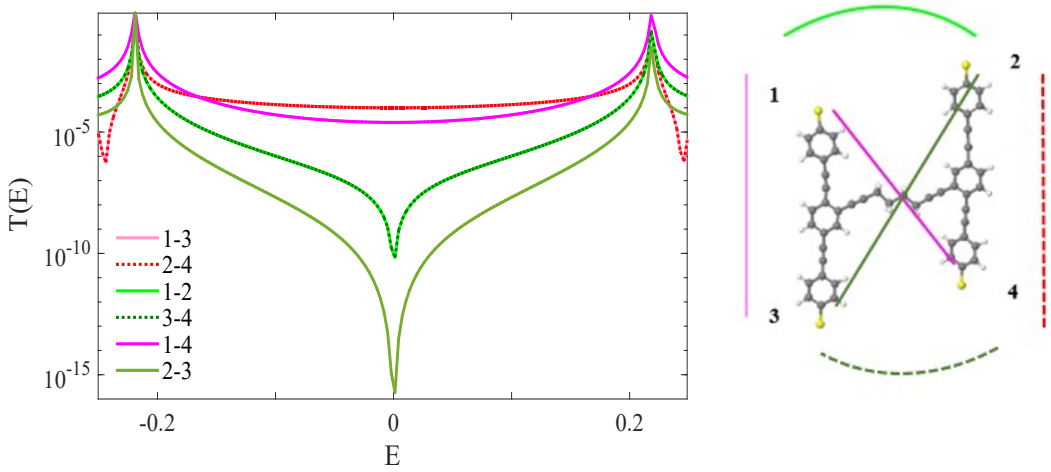

Figure S5: **Right panel:** Schematic illustration of C-L**1** in six contact points: (**1-3**), (**2-4**), (**1-2**), (**3-4**), (**1-4**), and (**2-3**). **Left panel**: transmission coefficients *T(E)* by TBM of C-L**1** against electron energy E.

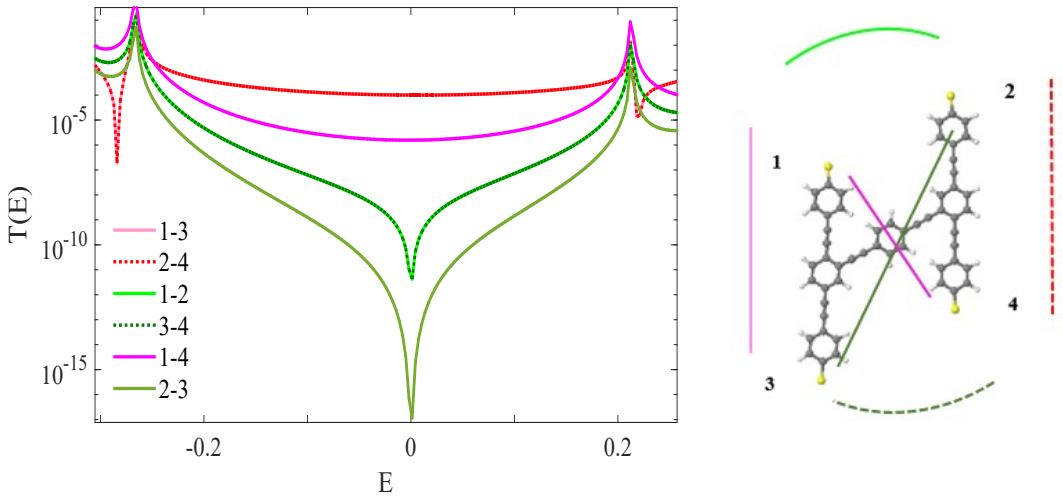

Figure S6: **Right panel:** Schematic illustration of C-L**2** in six contact points: (**1-3**), (**2-4**), (**1-2**), (**3-4**), (**1-4**), and (**2-3**). **Left panel**: transmission coefficients *T(E)* by TBM of C-L**2** against electron energy E.

4. Transport Simulations

In the following transport calculations, the ground state Hamiltonian and optimised geometry of each compound were obtained using the density functional theory (DFT) code. The local density approximation (GGA) exchange-correlation functional was used along with double zeta polarised (DZP) basis sets and the norm-conserving pseudopotentials. The real space grid was defined by a plane wave cut-off of 250 Ry. The geometry optimisation was carried out to a force tolerance of 0.01 eV/Å. This process was repeated for a unit cell with the molecule between two electrodes where the optimised distance between electrodes and the anchor groups. From the ground state Hamiltonian, the transmission coefficient, and the room temperature electrical conductance G was obtained, as described in the sections below. In this section, we shall calculate the transport in gold junctions as follows:

4.1 Transport Simulation in Au-Au Junction for cross-linked 1

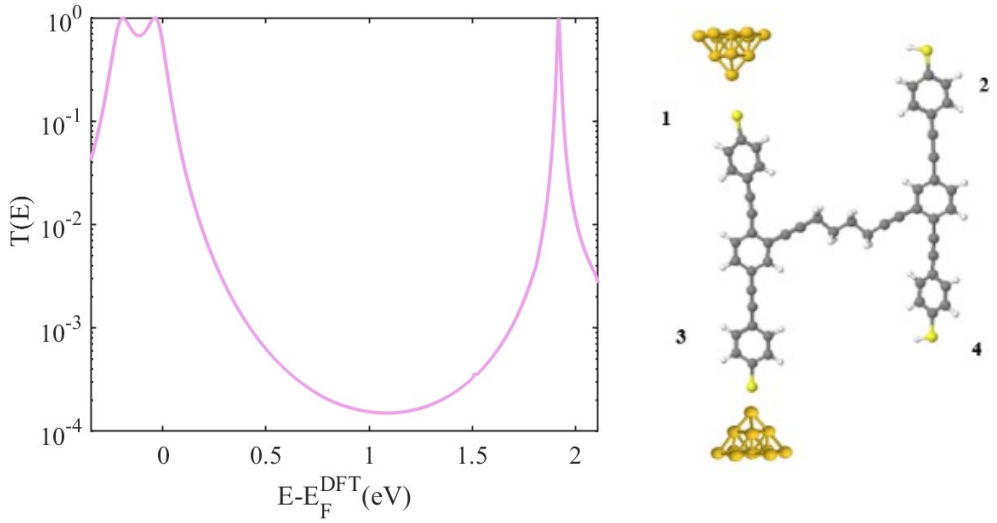

Figure S7: **Right panel**: Schematic illustration of the Au/C-L**1**/Au junctions in (**1-3**) contact points. **Left panel**: transmission coefficient *T(E)* of Au/C-L**1**/Au junctions against electron energy E.

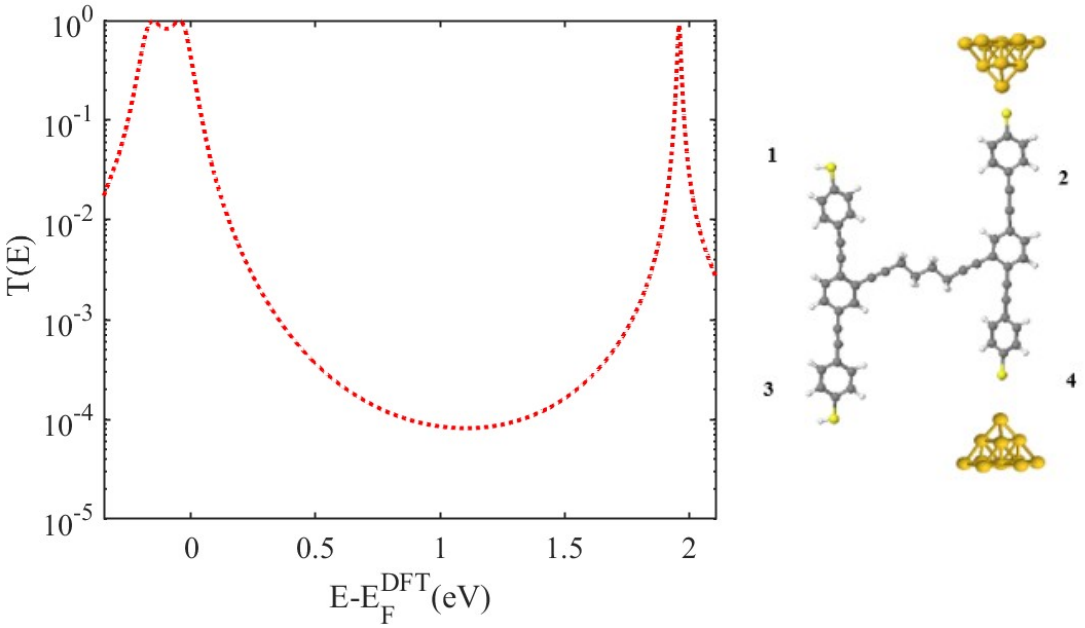

Figure S8: Right panel: Schematic illustration of the Au/C-L**1**/Au junctions in (**2-4**) contact points. **Left panel**: transmission coefficient *T(E)* of Au/C-L**1**/Au junctions against electron energy E.

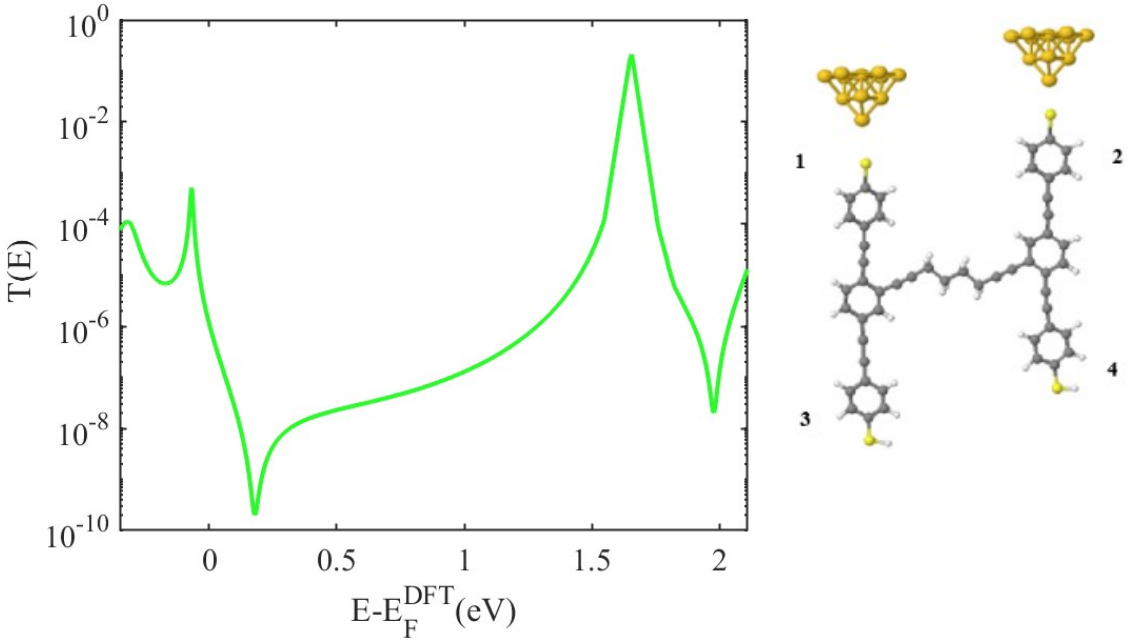

Figure S9: Right panel: Schematic illustration of the Au/C-L**1**/Au junctions in (**1-2**) contact points. **Left panel**: transmission coefficient *T(E)* of Au/C-L**1**/Au junctions against electron energy E.

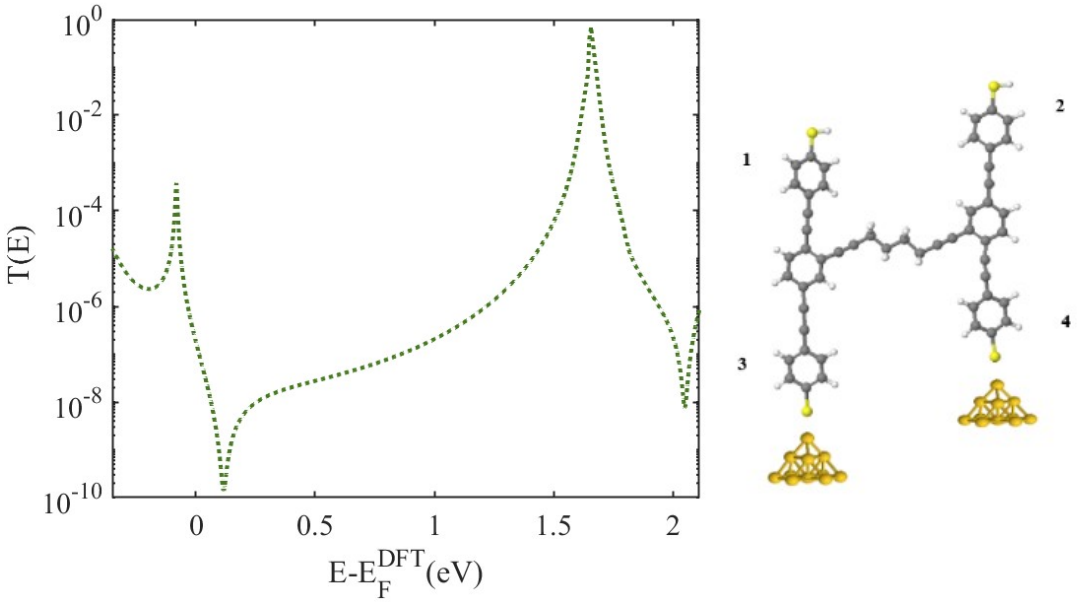

Figure S10: Right panel: Schematic illustration of the Au/C-L**1**/Au junctions in (**3-4**) contact points. **Left panel**: transmission coefficient *T(E)* of Au/C-L**1**/Au junctions against electron energy E.

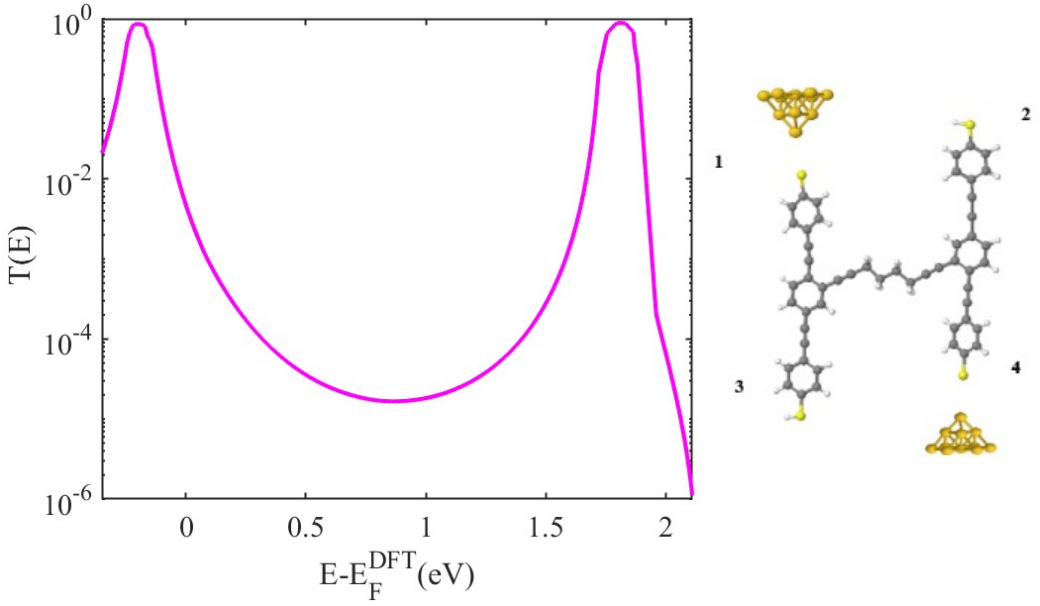

Figure S11: **Right panel**: Schematic illustration of the Au/C-L**1**/Au junctions in (**1-4**) contact points. **Left panel**: transmission coefficient *T(E)* of Au/C-L**1**/Au junctions against electron energy E.

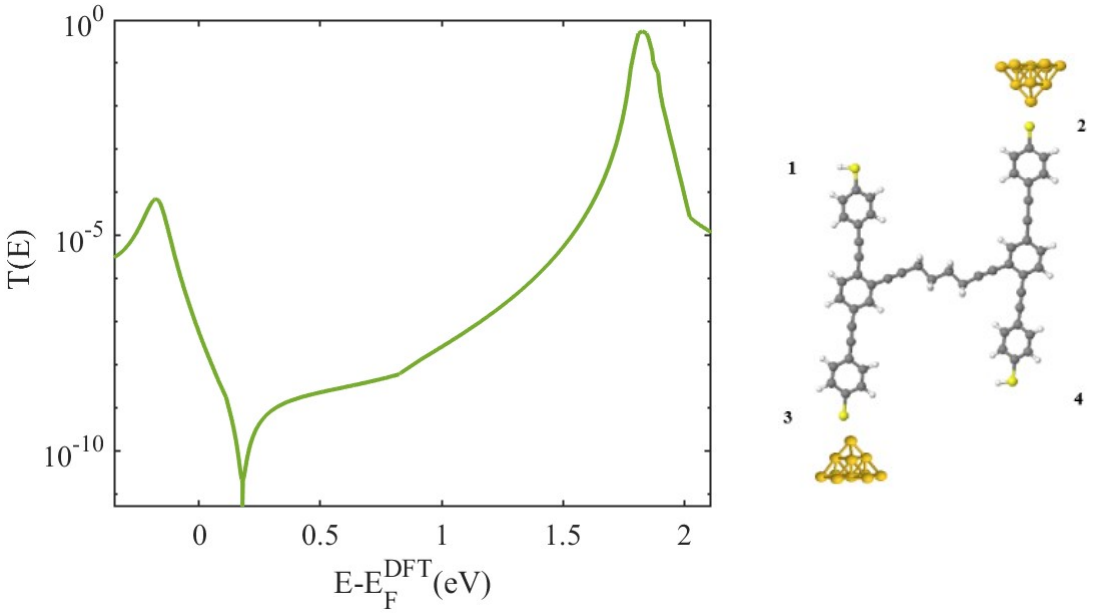

Figure S12: Right panel: Schematic illustration of the Au/C-L**1**/Au junctions in (**2-3**) contact points. **Left panel**: transmission coefficient T(E) of Au/C-L**1**/Au junctions against electron energy E.

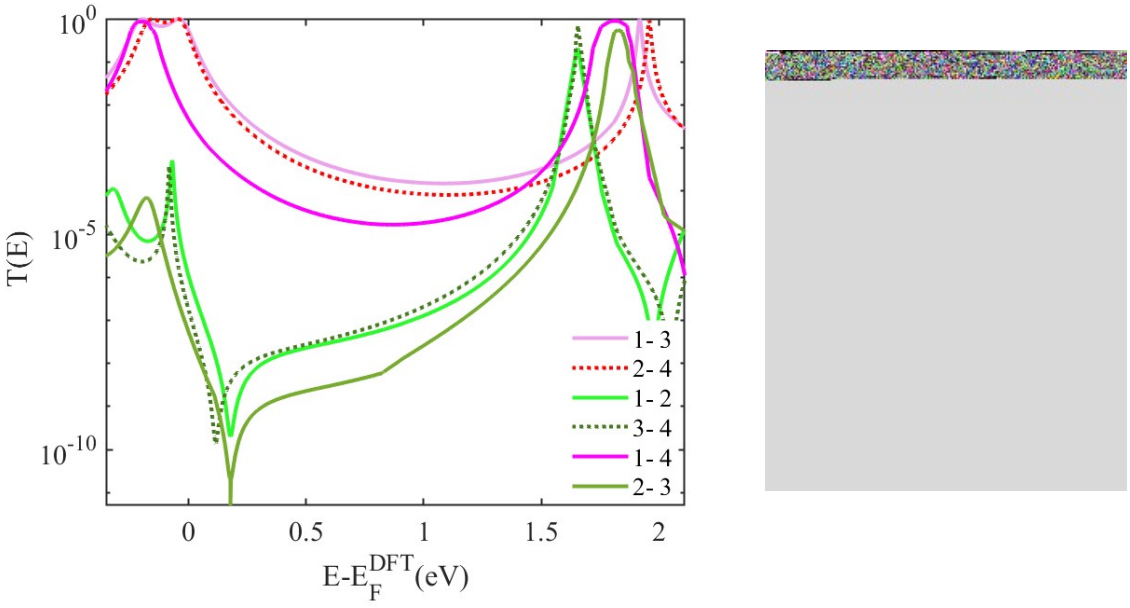

Figure S13: **Right panel:** Schematic illustration of the Au/C-L**1**/Au junctions in in six contact points: (**1-3**), (**2-4**), (**1-2**), (**3-4**), (**1-4**), and (**2-3**). **Left panel**: transmission coefficients *T(E)* of Au/C-L**1**/Au junctions against electron energy E.

4.2 Transport Simulation in Au-Au Junction for cross-linked 2

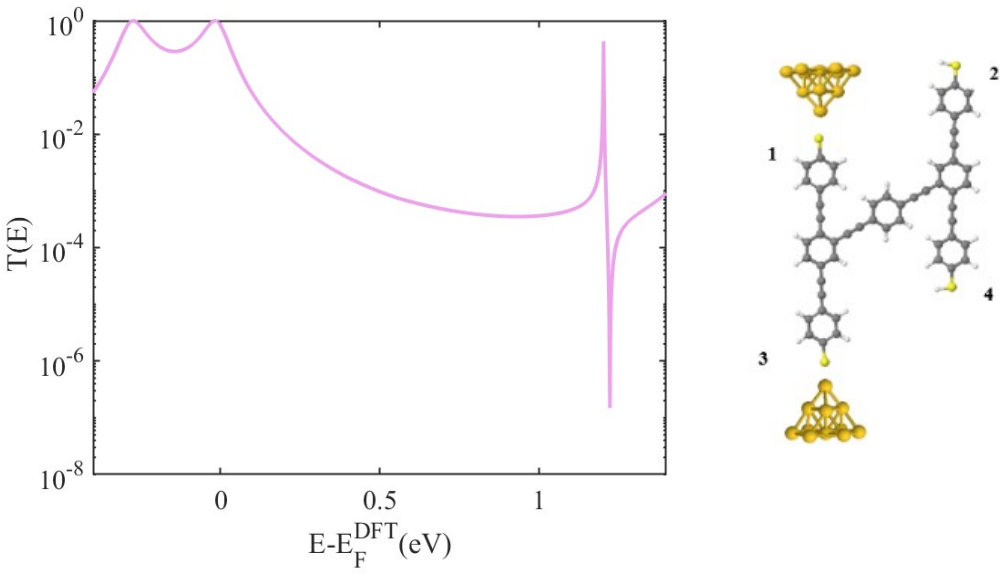

Figure S14: Right panel: Schematic illustration of the Au/C-L**2**/Au junctions in (**1**-**3**) contact points.
Left panel: transmission coefficient *T(E)* of Au/C-L**2**/Au junctions against electron energy E.

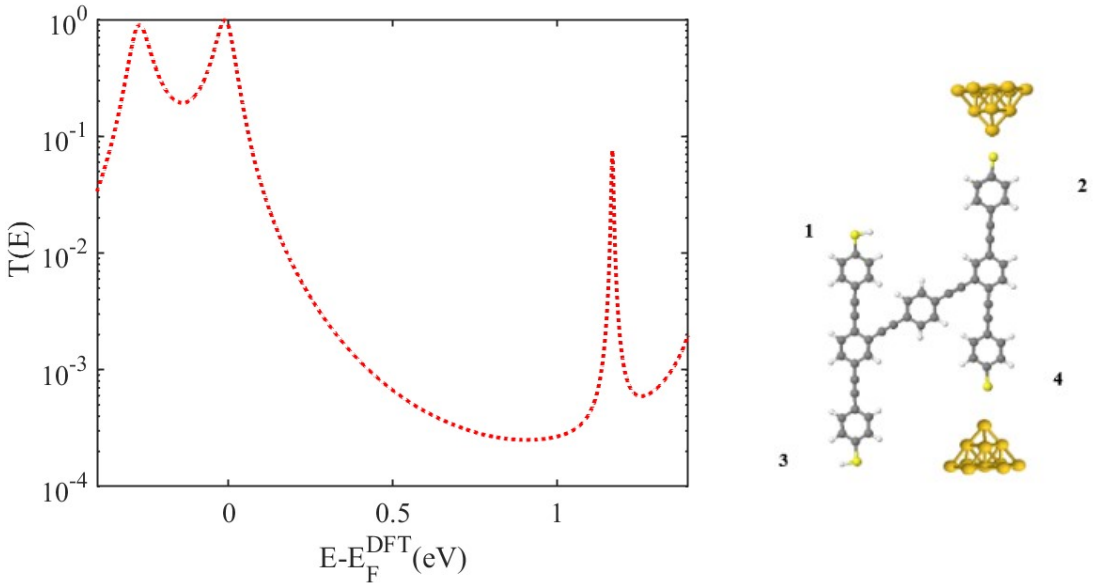

Figure S15: **Right panel**: Schematic illustration of the Au/C-L**2**/Au junctions in (**2**-**4**) contact points.
Left panel: transmission coefficient *T(E)* of Au/C-L**2**/Au junctions against electron energy E.

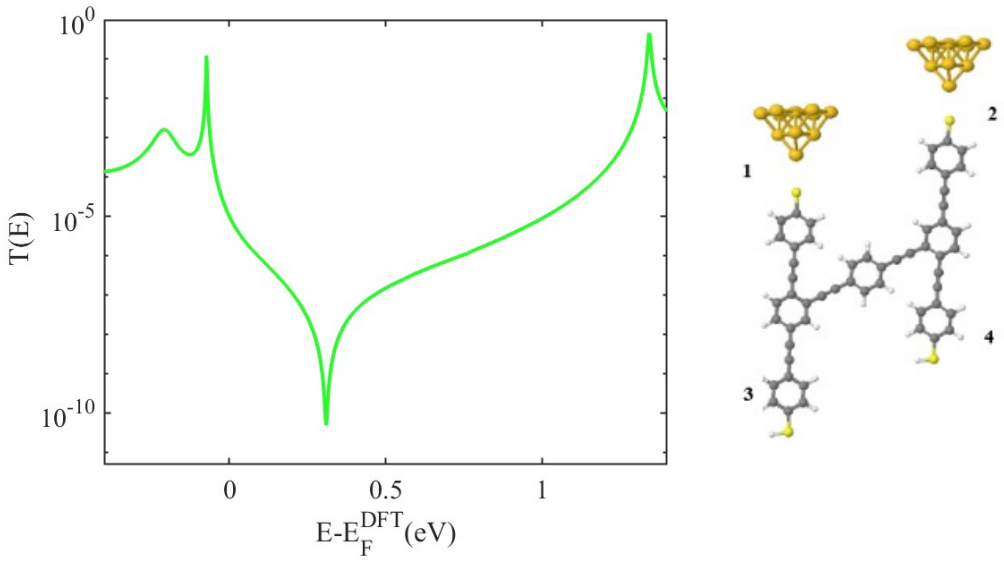

Figure S16: **Right panel**: Schematic illustration of the Au/C-L**2**/Au junctions in (**1-2**) contact points. **Left panel**: transmission coefficient *T(E)* of Au/C-L**2**/Au junctions against electron energy E.

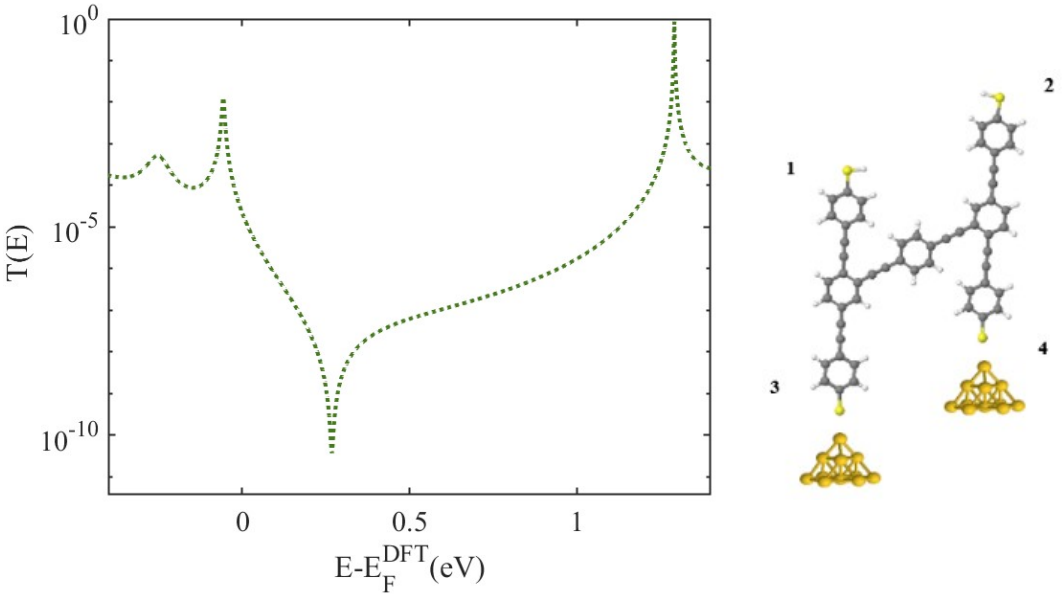

Figure S17: Right panel: Schematic illustration of the Au/C-L**2**/Au junctions in (**3-4**) contact points. **Left panel**: transmission coefficient *T(E)* of Au/C-L**2**/Au junctions against electron energy E.

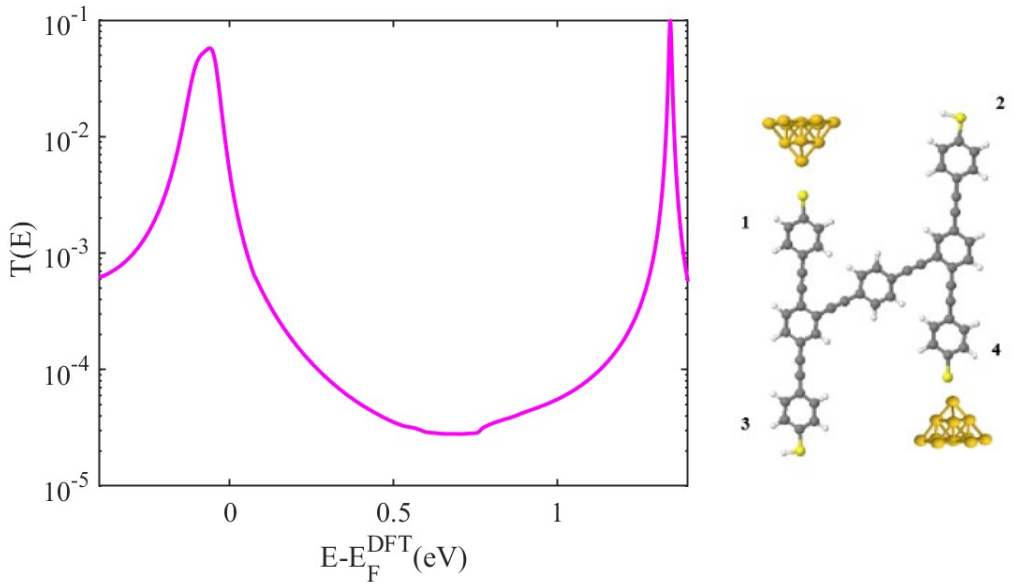

Figure S18: Right panel: Schematic illustration of the Au/C-L**2**/Au junctions in (**1-4**) contact points.
Left panel: transmission coefficient *T(E)* of Au/C-L**2**/Au junctions against electron energy E.

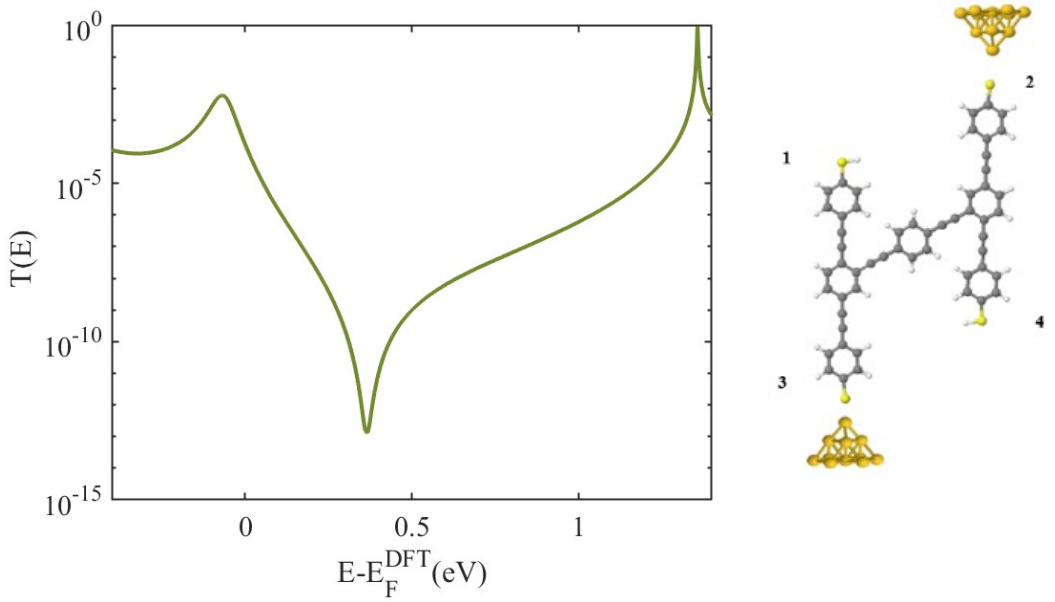

Figure S19: **Right panel**: Schematic illustration of the Au/C-L**2**/Au junctions in (**2-3**) contact points.
Left panel: transmission coefficient *T(E)* of Au/C-L**2**/Au junctions against electron energy E.

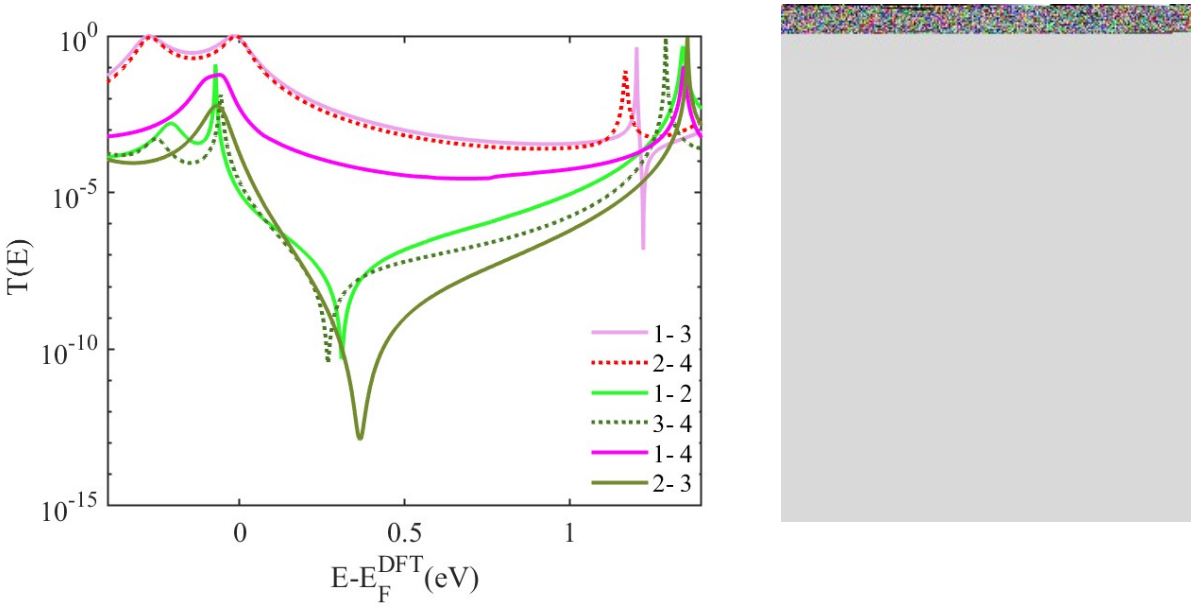

Figure S20: **Right panel:** Schematic illustration of the Au/C-L**2**/Au junctions in in six contact points: (**1-3**), (**2-4**), (**1-2**), (**3-4**), (**1-4**), and (**2-3**). **Left panel**: transmission coefficients *T(E)* of Au/C-L**2**/Au junctions against electron energy E.